Molecular Cell, Volume *28*

Supplemental Data

Structural Organization of the Anaphase-Promoting Complex Bound to the Mitotic Activator Slp1

Melanie D. Ohi, Anna Feoktistova, Liping Ren, Calvin Yip, Yifan Cheng, Jun-Song Chen, Hyun-Joo Yoon, Joseph S. Wall, Zhong Haung, Pawel A. Penczek, Kathleen L. Gould, and Thomas Walz

Supplemental Experimental Procedures

Analysis of Lid1-TAP Purifications by Mass Spectrometry

Lid1-TAP purifications from *mts3-1 and mts3-1 mad*Δ*2 mad3*Δ arrested cells were subjected to trypsin digestion and MudPIT mass spectrometric analysis as described (Yoon et al., 2002). The data were searched against the *S. pombe* protein database using Sequest (Thermo Finnigan) and were then processed with the TransProteomic Pipeline program (originally developed by ISB). The sequence coverage and number of unique peptides are shown in Figure 1A, S5A, and S7A.

Scanning Transmission EM (STEM)

STEM was carried out in the Brookhaven National Laboratory (BNL) STEM facility with tobacco mosaic virus (TMV) included as an internal control. For mass measurements, freeze-dried *S. pombe* APC/C particles were prepared by the wet film technique, as described on http://www.biology.bnl.gov/stem/stem.html under Specimen Preparation. Details of STEM and mass analysis are described (Wall et al., 1998; Wall and Simon, 2001). The program PCMass was used for these analyses.

Projection Analysis of Negatively Stained APC/C

3,027 pairs of conventionally negatively stained APC/C particles were selected interactively from untilted images (35 images) using WEB, the display program associated with SPIDER (Frank et al., 1996), and windowed into 120 x 120 pixel images. The particles selected from the images were rotationally and translationally aligned and subjected to 10 cycles of multi-reference alignment and K-means classification specifying 20 output classes (data not shown). The references used for the first multi-reference alignment were randomly chosen from the raw images. From the class averages, two representative projections were chosen and used as references for another cycle of multi-reference alignment (data not shown). The larger of the resulting two classes (2,334 particles) is shown in Figure 1S.

Supplemental References

Frank, J., Radermacher, M., Penczek, P., Zhu, J., Li, Y., Ladjadj, M., and Leith, A. (1996). SPIDER and WEB: processing and visualization of images in 3D electron microscopy and related fields. J Struct Biol *116*, 190-199.

Wall, J. S., Hainfeld, J. F., and Simon, M. N. (1998). Scanning transmission electron microscopy of nuclear structures. Methods Cell Biol *53*, 139-164.

Wall, J. S., and Simon, M. N. (2001). Scanning transmission electron microscopy of DNA-protein complexes. Methods Mol Biol *148*, 589-601.

Yoon, H. J., Feoktistova, A., Wolfe, B. A., Jennings, J. L., Link, A. J., and Gould, K. L. (2002). Proteomics analysis identifies new components of the fission and budding yeast anaphase-promoting complexes. Curr Biol *12*, 2048-2054.

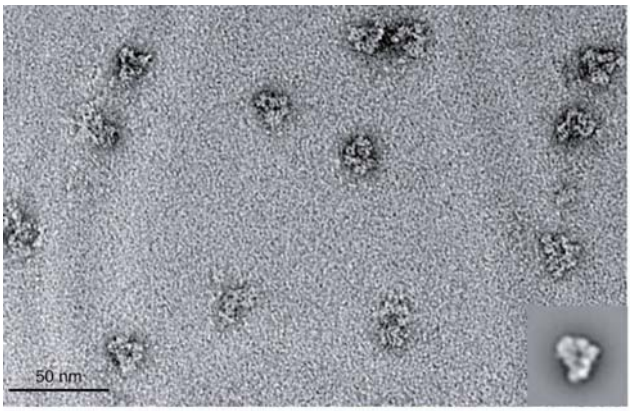

Figure S1. *S. pombe* APC/C Complex in Negative Stain

Negatively stained Lid1-TAP particles are structurally homogeneous as revealed by the average of 2,334 particles shown in the inset. Scale bar is 50 nm. Side length of the inset is 53.7 nm.

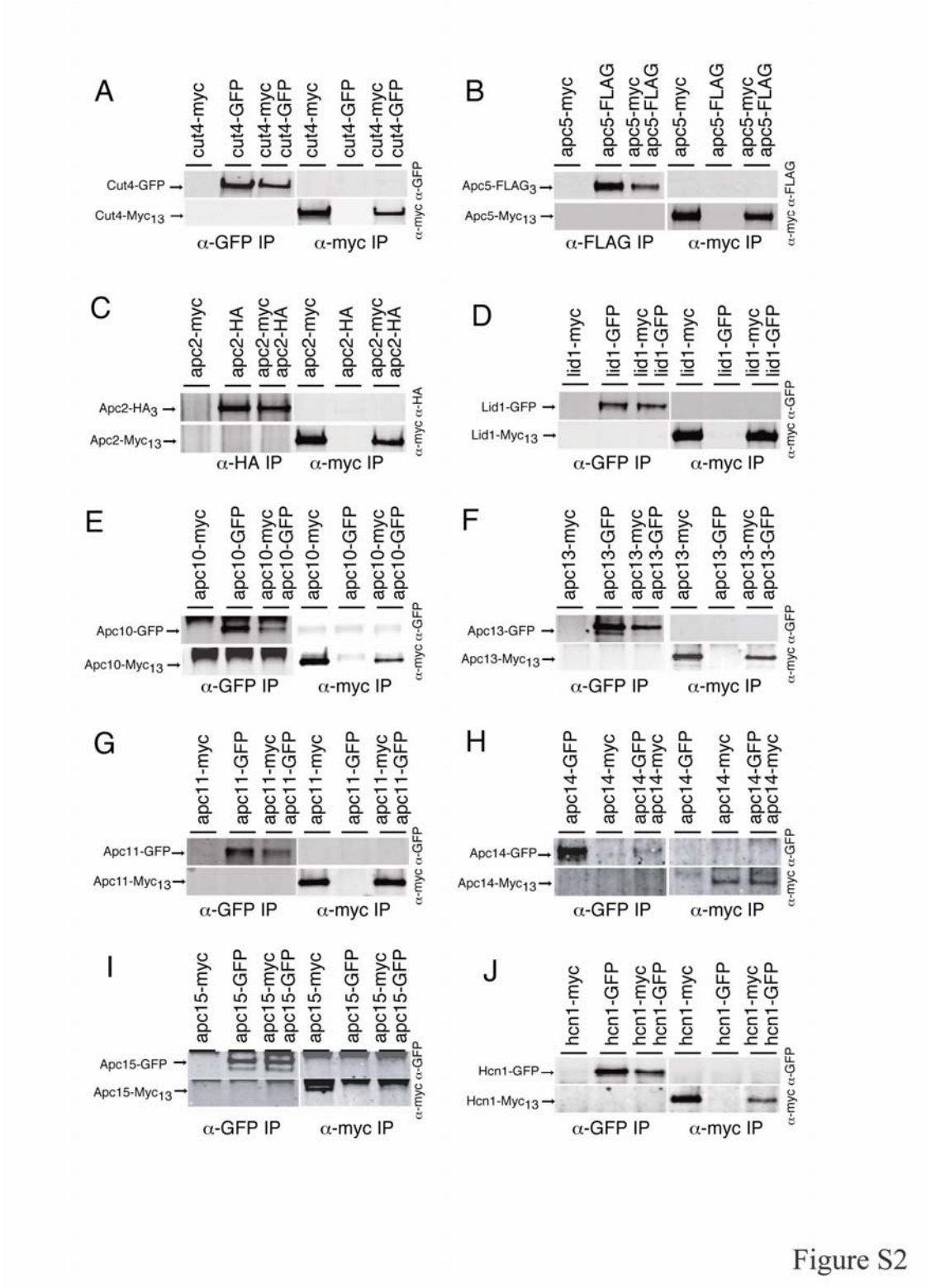

Figure S2. Determination of *S. pombe* APC/C Subunit Stoichiometry

Cut4, Apc5, Apc2, Lid1, Apc10, Acp13, Apc11, Apc14, Acp15, and Hcn1 do not self-associate *in vivo*.

(A) An anti-GFP (upper panel) and an anti-Myc (lower panel) immunoblot of immunoprecipitates from *cut4-GFP*, *cut4-Myc$_{13}$*, and *cut4-GFP cut4-Myc$_{13}$* strains. Immunoprecipitations were performed with anti-GFP or anti-Myc antibodies.

(B) An anti-FLAG (upper panel) and an anti-Myc (lower panel) immunoblot of immunoprecipitates from *apc5-Myc$_{13}$*, *apc5- flag$_3$*, and *apc5-Myc$_{13}$ apc5- flag$_3$* strains. Immunoprecipitations were performed with anti-FLAG or anti-Myc antibodies.

(C) An anti-HA (upper panel) and an anti-Myc (lower panel) immunoblot of immunoprecipitates from *apc2-Myc$_{13}$*, *apc2-HA$_3$,* and *apc2-Myc$_{13}$ apc2-HA$_3$* strains. Immunoprecipitations were performed with anti-HA or anti-Myc antibodies.

(D) An anti-GFP (upper panel) and an anti-Myc (lower panel) immunoblot of immunoprecipitates from *lid1-GFP*, *lid1-Myc$_{13}$*, and *lid1-GFP lid1-Myc$_{13}$* strains. Immunoprecipitations were performed with anti-GFP or anti-Myc antibodies.

(E) An anti-GFP (upper panel) and an anti-Myc (lower panel) immunoblot of immunoprecipitates from *apc10-GFP*, *apc10-Myc$_{13}$*, and *apc10-GFP apc10-Myc$_{13}$* strains. Immunoprecipitations were performed with anti-GFP or anti-Myc antibodies.

(F) An anti-GFP (upper panel) and an anti-Myc (lower panel) immunoblot of immunoprecipitates from *apc13-GFP*, *apc13-Myc$_{13}$*, and *apc13-GFP apc13-Myc$_{13}$* strains. Immunoprecipitations were performed with anti-GFP or anti-Myc antibodies.

(G) An anti-GFP (upper panel) and an anti-Myc (lower panel) immunoblot of immunoprecipitates from *apc11-GFP*, *apc11-Myc$_{13}$*, and *apc11-GFP apc11-Myc$_{13}$* strains. Immunoprecipitations were performed with anti-GFP or anti-Myc antibodies.

(H) An anti-GFP (upper panel) and an anti-Myc (lower panel) immunoblot of immunoprecipitates from *apc14-GFP*, *apc14-Myc$_{13}$*, and *apc14-GFP apc14-Myc$_{13}$* strains. Immunoprecipitations were performed with anti-GFP or anti-Myc antibodies. (I) An anti-GFP (upper panel) and an anti-Myc (lower panel) immunoblot of immunoprecipitates from *apc15-GFP*, *apc15-Myc$_{13}$*, and *apc15-GFP apc15-Myc$_{13}$* strains. Immunoprecipitations were performed with anti-GFP or anti-Myc antibodies. (J) An anti-GFP (upper panel) and an anti-Myc (lower panel) immunoblot of immunoprecipitates from *hcn1-GFP*, *hcn1-Myc$_{13}$*, and *hcn1-GFP hcn1-Myc$_{13}$* strains. Immunoprecipitations were performed with anti-GFP or anti-Myc antibodies.

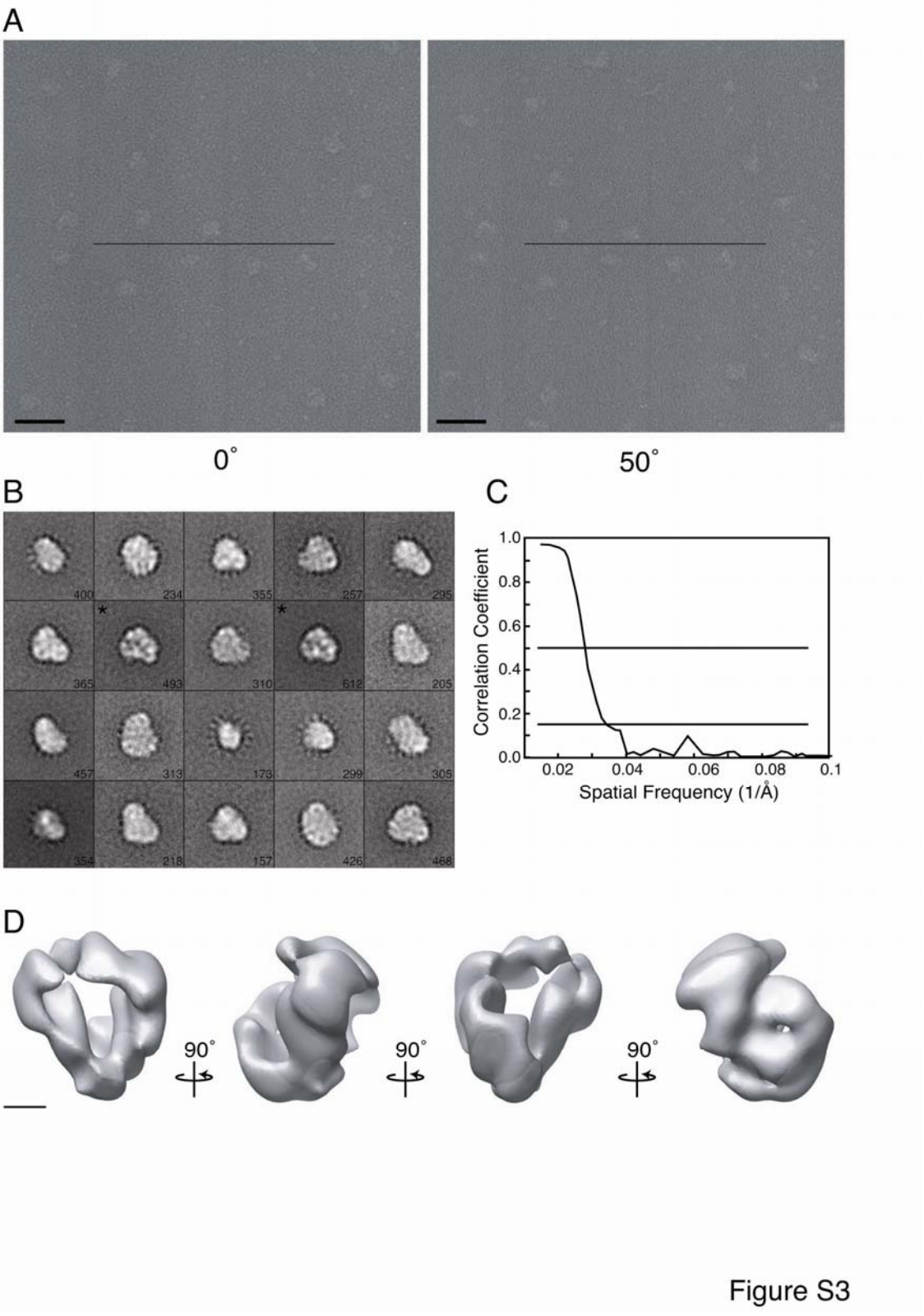

Figure S3. *S. pombe* APC/C in Cryonegative Stain

(A) Areas of typical electron micrographs of APC/C particles at 0˚ and 50˚ tilt prepared by cryo-negative staining. Line indicates tilt axis. Scale bar is 50 nm.

(B) Class averages obtained by multi-reference alignment and classification of 6,696 APC/C particle images into 20 classes. The number of particles in each projection average is shown in the lower right corner of each average. The two averages that were combined and used for 3D reconstruction are marked with a "*" in the upper left corner. Side length of individual panels is 50.4 nm.

(C) Fourier shell correlation (FSC) was used to estimate the resolution of the density map. The resolution is 36 Å at the FSC = 0.5 cut-off.

(D) 3D reconstruction of the APC/C in cryo-negative stain. A high threshold level was chosen for contouring to enhance the features present in the density map.

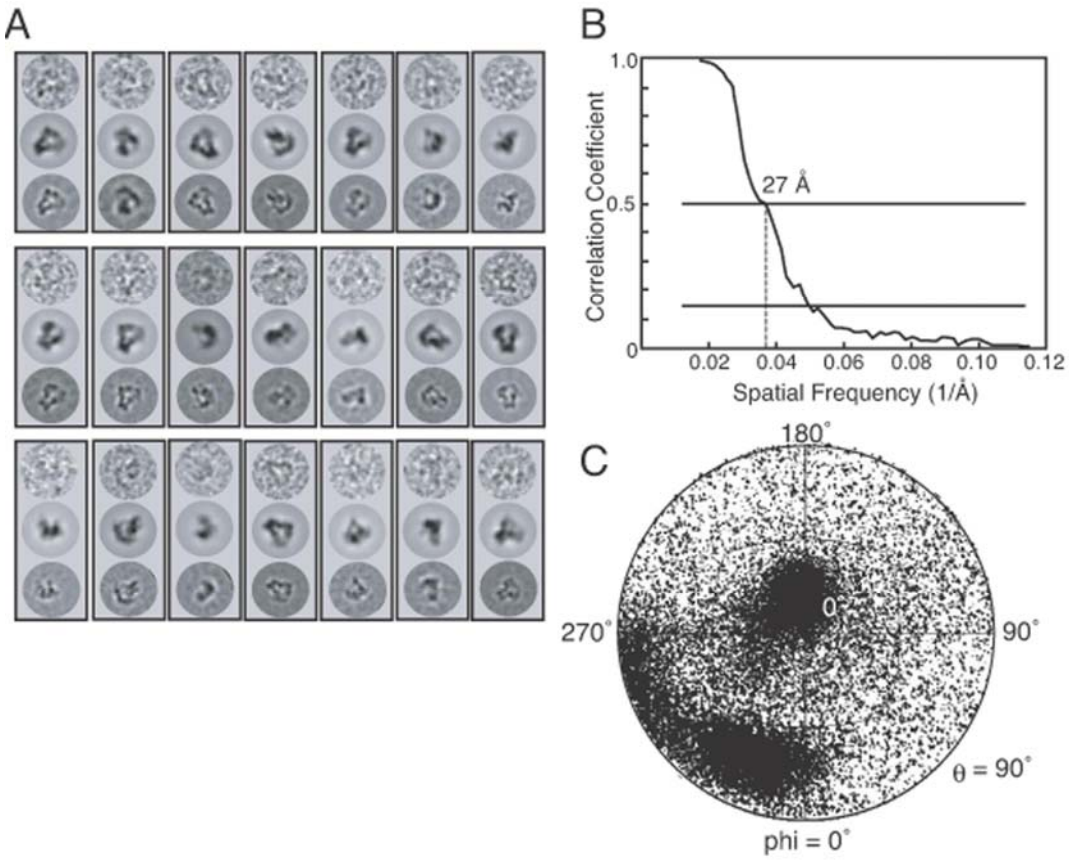

Figure S4. Image Analysis of the Vitrified *S. pombe* APC/C

(A) Selected raw particle images of the APC/C aligned with their best correlating reprojections of the density map shown in Figure 3 and with their respective class averages. Top panel: raw images; middle panel: reprojections from the 3D map (see Fig. 3); bottom panel: class averages. Each class average contains about 300 particles. Side length of panels is 50.4 nm.

(B) The resolution is 27.0 Å at a 0.5 cut-off. (C) Plot of the Euler angles for all the particles (28,540 particles) included in the 3D reconstruction, showing the orientations of the particles in the vitrified ice layer.

A

	lid1-TAP cut4-2xmyc	*lid1-TAP apc2-2xmyc*	*lid1-TAP nuc2-2xmyc*	*apc13-TAP lid1-2xmyc*	*lid1-TAP apc5-2xmyc*	*lid1-TAP cut9-2xmyc*	*lid1-TAP cut23-2xmyc*	*lid1-TAP hcn1-2xmyc*	*lid1-TAP apc14-2xmyc*	*lid1-TAP apc15-2xmyc*
Cut4	53.1	30.8	58.7	32.2	53.5	55.2	59.4	56.0	58.0	33.1
Apc2	68.7	27.9	73.7	37.6	62.1	62.0	70.0	69.0	72.5	34.1
Nuc2	74.0	46.0	81.7	34.3	69.3	65.7	76.8	81.1	75.9	45.9
Lid1	54.8	27.0	64.3	34.1	54.9	50.9	59.0	55.2	64.0	31.0
Apc5	63.5	30.9	71.6	37.7	63.5	67.3	70.6	68.8	71.9	31.2
Cut9	65.6	42.8	74.5	47.2	62.6	58.9	73.0	79.4	73.0	34.6
Cut23	66.2	38.2	73.5	42.1	63.2	63.5	71.0	58.4	64.6	48.7
Apc10	48.1	24.9	85.2	35.4	61.4	61.4	85.7	68.8	79.4	41.3
Apc11	25.5	25.5	71.3	25.5	71.3	71.3	71.3	39.4	71.3	25.5
Hcn1	95.0	78.8	81.3	90.0	81.3	81.3	81.3	53.8	81.3	81.3
Apc13	43.7	24.4	85.2	45.9	77.8	62.2	80.0	73.3	73.3	34.8
Apc14	71.0	50.5	78.5	53.3	89.7	86.9	89.7	69.2	57.9	35.5
Apc15	28.7	16.2	28.7	22.1	28.7	28.7	28.7	28.7	28.7	19.1
Slp1	65.6	15.0	71.1	24.8	69.3	49.0	71.3	54.3	75.0	20.9

B

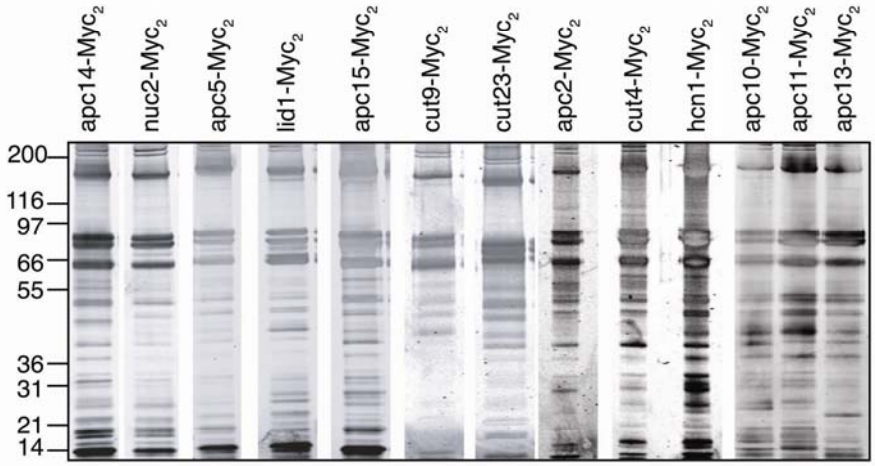

Figure S5. Composition of *S. pombe* APC/C Preparations Used in Antibody Labeling Experiments

(A) TAP/mass spectrometric results from APC/C particles that contain a Myc_2 epitope tagged copy of Cut4, Apc2, Nuc2, Lid1, Apc5, Cut9, Cut23, Hcn1, Apc14, or Apc15. Numbers represent the percent sequence coverage for each protein.

(B) Silver-stained gels of a portion of the Lid1-TAP or Apc13-TAP complexes that contain a Myc_2 epitope tagged copy of Apc14, Nuc2, Apc5, Lid1, Apc15, Cut9. Cut23, Apc2, Cut4, Hcn1, Apc10, Apc11, or Apc13.

A

	lid1-TAP slp1-HA	*lid1-TAP slp1-362*
Cut4	53.7	47.0
Apc2	63.9	51.5
Nuc2	69.0	64.1
Lid1	55.9	44.5
Apc5	67.3	54.5
Cut9	69.4	56.8
Cut23	63.7	59.1
Apc10	79.4	65.1
Apc11	71.3	25.5
Hcn1	81.3	81.3
Apc13	71.1	68.9
Apc14	83.2	75.7
Apc15	28.7	28.7
Slp1	51.4	0

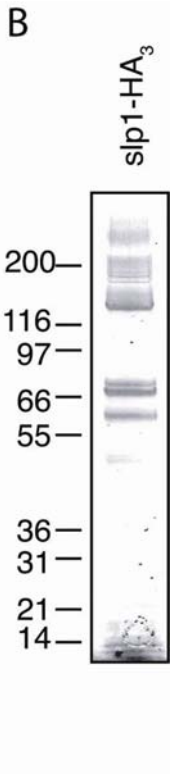

Figure S6. Composition of the *S. pombe* APC/C Purifications Used to Localize Slp1

(A) TAP/mass spectrometric results from APC/C particles that either contain a HA_3 epitope tagged copy of Slp1 or were purified from *slp1-362* cells. Numbers represent the percent sequence coverage for each protein.

(B) Silver-stained gel of a portion of the APC/C that contains a HA_3 epitope tagged copy of Slp1.

Table S1. *S. pombe* Strains Used in This Study

Strain	Genotype	Source
KGY24	*apc2-HA$_3$::Kan^R ade6-M210 ura4-D18 leu1-32* h$^-$	Lab stock
KGY33	*cut23-myc$_{13}$::Kan^R ade6-M210 ura4-D18 leu1-32* h$^-$	Lab stock
KGY48	*apc10-myc$_{13}$::Kan^R ade6-M210 ura4-D18 leu1-32* h$^-$	Lab stock
KGY51	*cut4-myc$_{13}$::Kan^R ade6-M210 ura4-D18 leu1-32* h$^-$	Lab stock
KGY88	*apc11-myc$_{13}$::Kan^R ade6-M210 ura4-D18 leu1-32* h$^-$	Lab stock
KGY246	*ade6-M210 ura4-D18 leu1-32* h$^-$	Lab stock
KGY1533	*apc14-myc$_{13}$::Kan^R ade6-M210 ura4-D18 leu1-32* h$^+$	Lab stock
KGY1549	*hcn1-GFP::Kan^R/hcn1-myc$_{13}$::Kan^R ade6-M210/ade6-M216 ura4-D18/ura4-D18 leu1-32/leu1-32* h$^-$/ h$^+$	Lab stock
KGY1560	*lid1-TAP::Kan^R apc2-myc$_2$::Kan^R mts3-1 ade6-M210 ura4-D18 leu1-32* h$^+$	This study
KGY1886	*hcn1-GFP::Kan^R ade6-M210 ura4-D18 leu1-32* h$^-$	Lab stock
KGY2049	*lid1-GFP::Kan^R ade6-M210 ura4-D18 leu1-32* h$^-$	Lab stock
KGY2050	*lid1-TAP::Kan^R mts3-1 mad2::ura4$^+$ mad3::ura4$^+$ ade6-M210 ura4-D18 leu1-32* h$^-$	This study
KGY2303	*lid1-TAP::Kan^R apc10-myc$_2$::Kan^R mts3-1 ura4-D18 leu1-32* h$^-$	This study
KGY3399	*hcn1- myc$_{13}$::Kan^R ade6-M210 ura4-D18 leu1-32* h$^-$	Lab stock
KGY3404	*nuc2-HA$_3$::Kan^R ade6-M210 ura4-D18 leu1-32* h$^-$	Lab stock
KGY3654	*lid1-TAP::Kan^R mts3-1 ura4-D18 leu1-32* h$^-$	This study
KGY3751	*apc15-myc$_{13}$::Kan^R ade6-M210 ura4-D18 leu1-32* h$^+$	Lab stock
KGY3862	*apc13-GFP::Kan^R ade6-M210 ura4-D18 leu1-32* h$^-$	Lab stock
KGY3978	*lid1-TAP::Kan^R nuc2-myc$_2$::Kan^R mts3-1 ura4-D18 leu1-32* h$^-$	This study
KGY4353	*lid1-TAP::Kan^R slp1-HA$_3$::Kan^R mts3-1 ade6-M210 ura4-D18 leu1-32* h$^-$	This study
KGY4875	*lid1-TAP::Kan^R apc11-myc$_2$::Kan^R mts3-1 ade6-M210 ura4-D18 leu1-32 mad2::ura4$^+$ mad3::ura4$^+$* h$^-$	This study
KGY4879	*lid1-TAP::Kan^R apc13-myc$_2$::Kan^R mts3-1 ade6-M210 ura4-D18 leu1-32 mad2::ura4$^+$ mad3::ura4$^+$* h$^+$	This study
KGY5396	*lid1-TAP::Kan^R mts3-1 cut9-HA$_3$::Kan^R ade6-M210 ura4-D18 leu1-32 mad2::ura4$^+$ mad3::ura4$^+$*h$^-$	This study
KGY5397	*lid1-TAP::Kan^R mts3-1 cut9-HA$_3$::Kan^R ura4-D18 leu1-32* h$^-$	This study
KGY5934	*lid1-TAP::Kan^R cut4-myc$_2$::Kan^R mts3-1 ura4-D18 leu1-32* h$^+$	This study
KGY6011	*lid1-TAP::Kan^R hcn1-myc$_2$::Kan^R mts3-1 ade6-M210 ura4-D18 leu1-32* h$^-$	This study
KGY6086	*apc2-myc$_{13}$::Kan^R ade6-M216 ura4-D18 leu1-32* h$^+$	This study
KGY6087	*apc10-GFP::Kan^R ade6-M216 ura4-D18 leu1-32* h$^+$	This study

KGY6088	*apc11-GFP::Kan^R ade6-M216 ura4-D18 leu1-32* h$^+$	This study
KGY6089	*apc13-myc$_{13}$::Kan^R ade6-M216 ura4-D18 leu1-32* h$^+$	This study
KGY6090	*cut4-GFP::Kan^R ade6-M216 ura4-D18 leu1-32* h$^+$	This study
KGY6096	*apc2-HA$_3$::Kan^R/apc2-myc$_{13}$::Kan^R ade6-M210/ade6-M216 ura4-D18/ura4-D18 leu1-32/leu1-32* h$^-$/ h$^+$	This study
KGY6097	*lid1-GFP::Kan^R/lid1- myc$_{13}$::Kan^R ade6-M210/ade6-M216 ura4-D18/ura4-D18 leu1-32/leu1-32* h$^-$/ h$^+$	This study
KGY6098	*apc13-GFP::Kan^R/ apc13-myc$_{13}$::Kan^R ade6-M210/ade6-M216 ura4-D18/ura4-D18 leu1-32/leu1-32* h$^-$/ h$^+$	This study
KGY6099	*apc10-myc$_{13}$::Kan^R/apc10-GFP::Kan^R ade6-M210/ade6-M216 ura4-D18/ura4-D18 leu1-32/leu1-32* h$^-$/ h$^+$	This study
KGY6100	*cut4- myc$_{13}$::Kan^R/cut4-GFP::Kan^R ade6-M210/ade6-M216 ura4-D18/ura4-D18 leu1-32/leu1-32* h$^-$/ h$^+$	This study
KGY6101	*apc11-myc$_{13}$::Kan^R/apc11-GFP::Kan^R ade6-M210/ade6-M216 ura4-D18/ura4-D18 leu1-32/leu1-32* h$^-$/ h$^+$	This study
KGY6145	*lid1-myc$_{13}$::Kan^R ade6-M216 ura4-D18 leu1-32* h$^+$	This study
KGY6178	*cut9-GFP::Kan^R ade6-M210 ura4-D18 leu1-32* h$^-$	This study
KGY6179	*cut9-flag$_3$::Kan^R ade6-M216 ura4-D18 leu1-32* h$^+$	This study
KGY6181	*cut23-GFP::Kan^R ade6-M216 ura4-D18 leu1-32* h$^+$	This study
KGY6189	*cut9-GFP::Kan^R/cut9-flag$_3$::Kan^R ade6-M210/ade6-M216 ura4-D18/ura4-D18 leu1-32/leu1-32* h$^-$/ h$^+$	This study
KGY6191	*cut23-myc$_{13}$::Kan^R/cut23-GFP::Kan^R ade6-M210/ade6-M216 ura4-D18/ura4-D18 leu1-32/leu1-32* h$^-$/h$^+$	This study
KGY6204	*lid1-TAP::Kan^R cut23-myc$_2$::Kan^R mts3-1 ade6-M210 ura4-D18 leu1-32* h$^-$	This study
KGY6205	*lid1-TAP::Kan^R cut9-myc$_2$::Kan^R mts3-1 ura4-D18 leu1-32* h$^+$	This study
KGY6232	*apc5- flag$_3$::Kan^R ade6-M210 ura4-D18 leu1-32* h$^-$	This study
KGY6293	*lid1-TAP::Kan^R slp1-362 mts3-1 ade6-M210 ura4-D18 leu1-32* h$^-$	This study
KGY6294	*apc13-TAP::Kan^R lid1-myc$_2$::Kan^R mts3-1 leu1-32* h$^-$	This study
KGY6300	*nuc2- myc$_{13}$::Kan^R ade6-M216 ura4-D18 leu1-32* h$^+$	This study
KGY6315	*lid1-TAP::Kan^R apc15-myc$_2$::Kan^R mts3-1 ade6-M210 ura4-D18 leu1-32* h$^-$	This study
KGY6316	*lid1-TAP::Kan^R apc5-myc$_2$::Kan^R mts3-1 ade6-M210 ura4-D18 leu1-32* h$^-$	This study
KGY6322	*apc15-GFP::Kan^R ade6-M216 ura4-D18 leu1-32* h$^-$	This study
KGY6331	*apc5- flag$_3$::Kan^R/apc5- myc$_{13}$::Kan^R ade6-M210/ade6-M216 ura4-D18/ura4-D18 leu1-32/leu1-32* h$^-$/ h$^+$	This study
KGY6333	*apc15-myc$_{13}$::Kan^R/apc15-GFP::Kan^R ade6-M210/ade6-M216 ura4-D18/ura4-D18 leu1-32/leu1-32* h$^-$/h$^+$	This study
KGY6334	*apc5- myc$_{13}$::Kan^R ade6-M216 ura4-D18 leu1-32* h$^+$	This study
KGY6336	*nuc2-HA$_3$::Kan^R/nuc2-myc$_{13}$::Kan^R ade6-M210/ade6-M216 ura4-D18/ura4-D18 leu1-32/leu1-32* h$^-$/h$^+$	This study
KGY6386	*apc14-myc$_{13}$::Kan^R/apc14-HA$_3$::Kan^R ade6-M210/ade6-M216 ura4-D18/ura4-D18 leu1-32/leu1-32* h$^-$/h$^+$	This study

KGY6388	*apc14-HA$_3$::Kan^R ade6-M216 ura4-D18 leu1-32* h$^-$	This study
KGY6389	*lid1-myc$_{13}$:: Kan^R cut4- flag$_3$::Kan^R cut9- flag$_3$::Kan^R ade6-M210 leu1-32* h$^+$	This study
KGY6390	*lid1-myc$_{13}$:: Kan^R cut4- flag$_3$::Kan^R cut23- flag$_3$::Kan^R ade6-M210 ura4-D18 leu1-32* h$^-$	This study
KGY6391	*lid1-myc$_{13}$:: Kan^R cut4- flag$_3$::Kan^R apc5- flag$_3$::Kan^R ade6-M210 ura4-D18 leu1-32* h$^+$	This study
KGY6445	*lid1-GFP::Kan^R cut4- myc$_{13}$::Kan^R nuc2- myc$_{13}$::Kan^R ade6-M210 ura4-D18 leu1-32* h$^+$	This study